Journal of Engineering Physics and Thermophysics, Vol. 70, No. 1, 1997

INFLUENCE OF STEFAN FLOW ON THE CHARACTERISTICS OF HETEROGENEOUS COMBUSTION OF A CARBON PARTICLE IN AIR*

V. V. Kalinchak, S. G. Orlovskaya,
A. I. Kalinchak, and A. V. Dubinskii

UDC 536.46:662.612

The influence of Stefan flow and radiation-induced heat losses on the characteristics of stationary high-and low-temperature stable and critical regimes of heat and mass transfer of a carbon particle in air is analyzed.

The influence of Stefan flow is, as a rule, ignored in considerations and analyses of high- and low-temperature states, their steadiness and critical conditions of heat and mass transfer for a carbon particle [1-3]. In [2, 3], it is shown that radiation-induced heat exchange of a particle with the cold walls of a reaction chamber creates the upper limit of particle sizes, above which no transition to the quasistationary high-temperature regime can proceed. Radiation heat losses are responsible for the fact that in the range of large sizes the critical diameter at which a particle ignites increases with its initial temperature. It is proved that radiation heat losses specify the critical gas temperature below which it is impossible to reach a quasistationary high-temperature regime in heat and mass transfer (HMT) merely by changing the particle diameter and initial temperature.

Below we analyze the influence of Stefan flow on the characteristics of heterogeneous combustion and oxidation, critical conditions of ignition, and spontaneous and forced extinction of a carbon particle. The heat exchange between the particle and the walls of the reaction chamber is taken into consideration. At Bi < 1, the equations of heat and mass balance for a carbon particle, provided that two concurrent reations proceed on its surface, with allowance for Stefan flow are as follows [4]:

$$\frac{1}{6} c_1 \rho_1 d \frac{dT_1}{dt} = Q_{ch} - Q_{h.r}, \quad T_1 (t = 0) = T_{in}, \tag{1}$$

where

$$Q_{ch} = \sum_{i=1}^{2} (k_i q_i) \rho_2 C_{1\infty} \left[\frac{k_{eff}}{\beta} + 1\right]^{-1}; \quad Q_{h.r} = Q_{\lambda,sf} + Q_r, \quad Q_{\lambda,sf} = Q_\lambda + Q_{sf};$$

$$Q_\lambda = \alpha (T_1 - T_2) = \frac{2\lambda_2}{d} (T_1 - T_2); \quad Q_{sf} = \frac{1}{2} c_2 \rho_2 P_{sf} \left[\frac{k_{eff}}{\beta} + 1\right]^{-1} (T_1 + T_2);$$

$$k_{eff} = \sum_{i=1}^{2} k_i + P_{sf}, \quad k_i + k_{0i} \exp\left(-\frac{E_i}{RT_1}\right),$$

$i = 1$ – the reaction $C + O_2 \rightarrow CO_2$ (I), $i = 2$ – the reaction $2C + O_2 \rightarrow 2CO$ (II);

$$P_{sf} = \frac{\mu_S}{\mu_1} \left(\sum_{i=1}^{2} k_i + k_2\right) C_{1\infty}; \quad \beta = \frac{2D}{d},$$

* The investigations are sponsored by the International Fund "Vidrodzhennya" within the framework of the program ISSEP (contract No. K6V100).

Odessa I. I. Mechnikov State University, Ukraine. Translated from Inzhenerno-Fizicheskii Zhurnal, Vol. 70, No. 1, pp. 146-152, January-February, 1997. Original article submitted August 22, 1994.

 1062-0125/97/7001-0150$18.00

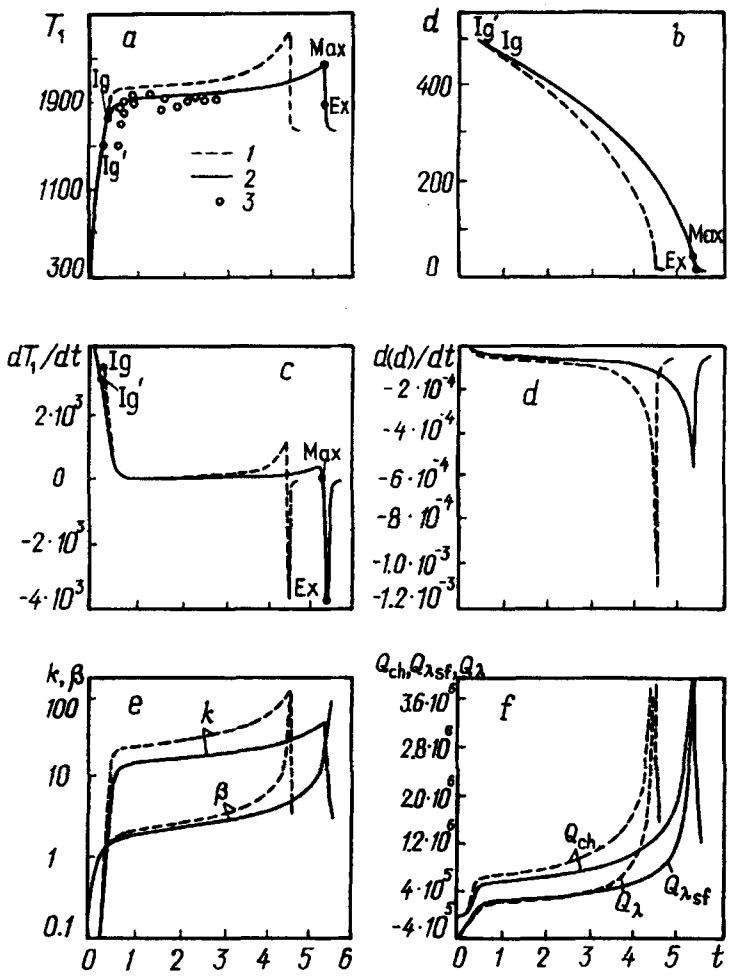

Fig. 1. Plots of $T_1(t)$ (a); $d(t)$ (b), $dT_1/dt(t)$ (c); $d(d)/dt(t)$ (d); $k(t)$, $\beta(t)$ (e); $Q_{ch}(t)$, $Q_{\lambda,sf}(t)$, $Q_\lambda(t)$ (f) at $T_2 = T_w = 1600$ K; $C_{1\infty} = 0.23$; $T_{in} = 300$ K; $d_{in} = 500$ μm; 1) $P_{sf} = 0$; 2) $P_{sf} \neq 0$; 3) experiment [5]. T, K; t, sec; d, μm; dT_1/dt, K/sec; $d(d)/dt$, m/sec; k, β, m/sec; Q, W/m^2.

$$\frac{d(d)}{dt} = -\frac{2\rho_2}{\rho_1}\sum_{i=1}^{2}(\Omega_i k_i)\, C_{1\infty}\left(\frac{k_{eff}}{\beta}+1\right)^{-1}, \quad d(t=0) = d_{in}. \tag{2}$$

Equations (1) and (2) make it possible to analyze the influence of Stefan flow on the characteristics of stationary high- and low-temperature states as well as the critical HMT conditions that determine heterogeneous ignition and extinction of a carbon particle.

To determine the time required for developing a high-temperature regime (the induction period), the combustion time, and the critical parameters of extinction, the method developed in [3] can be used. Figure 1 shows plots of $T_1(t)$; $d(t)$; $dT_1/dt(t)$; $d(d)/dt(t)$; $k(t)$, where k is the total rate constant of chemical reactions $k\sum_{i=1}^{2} k_i$; $\beta(t)$; $Q_{ch}(t)$, $Q_{\lambda,sf}(t)$, $Q_\lambda(t)$ are determined from Eqs. (1) and (2) at an air temperature higher than its critical value, with and without regard for Stefan flow for the carbon particle (anthracene coke). Calculations are made at the following physicochemical parameters: $E_1 = 140{,}030$ J/mole, $E_2 = 154{,}000$ J/mole; $k_{01} = 45{,}000$ m/sec, $k_{02} = 130{,}030$ m/sec, $q_1 = 10.125 \cdot 10^6$ J/(kg·O$_2$), $q_2 = 6.8 \cdot 10^6$ J/(kg·O$_2$) [6].

The induction period is defined as the time required to reach a quasistationary high-temperature regime in the processes of HMT and chemical kinetics. The first minimum on the curve of dT_1/dt ($dT_1/dt > 0$) (Figs. 1a and 1c) indicates completion of the first stage, which is characterized by heat removal $Q_{ch} \approx 0$ and a kinetic reaction

TABLE 1. Characteristics of Ignition, Combustion and Extinction of a Particle with $d_{in} = 200\ \mu m$ at $T_2 = 1400$ K, $T_w = 500$ K with ($P_{sf} \neq 0$) and without ($P_{sf} = 0$) Regard for Stefan Flow

P_{sf}	t_{ind}, sec	t_{com}, sec	T_{1Max}, K	d_{Ex}, μm
$P_{sf} = 0$	0.417	0.738	2238	30.7
$P_{sf} \neq 0$	0.795	0.898	1836	73.4

mode ($k \ll \beta$). This stage is marked by the point Ig'. At this stage the particle diameter is practically unchanged and the reaction rate is low (Figs. 1b and 1d). At the second stage, with an increase in Q_{ch} and Stefan flow, a transition to the high-temperature regime occurs. In this case, the total rate constant of the chemical reaction becomes equal to β. At the point Ig, the positive value of the time-dependent derivative of the particle temperature reaches its maximum and a transition to the quasistationary regime of combustion occurs. The point Ig, at which $dT_1/dt > 0$, $d^2T_1/dt^2 = 0$, and $d^3T_1/dt^3 < 0$, determines the induction period of heterogeneous particle ignition t_{ind}. In the case of particle combustion $dT_1/dt \simeq 0$, the total rate constant of the reactions is insignificantly higher than the mass transfer coefficient ($k/\beta \approx 4-5$), which does not allow us to consider the combustion regime as a diffusional one.

After the combustion temperature of the particle passes through its maximum, it decreases (the point Max, Fig. 1a). Such a trend of $T_1(t)$ is due to the different degrees of the particle-diameter effect on Q_{ch} and $Q_{\lambda,sf}$ with allowance for radiation heat losses. In the region of large diameters, where Q_r is relatively great, a decrease in the particle diameter with time causes a higher increase in Q_{ch} as compared to $Q_{\lambda,sf}$. In the region of small diameters, the radiation heat losses decrease as compared to $Q_{\lambda,sf}$. A decrease in the particle diameter results in a higher, as compared to Q_{ch}, increase in $Q_{\lambda,sf}$. This entails a decrease in the combustion temperature after passage through its maximum. When the particle diameter and temperature reach their critical values (the point Ex), a spontaneous transition from a quasistationary high-temperature to a low-temperature regime occurs. At the moment of extinction t_{Ex} the negative value of the time-dependent derivative of the particle temperature acquires a minimum value ($dT_1/dt < 0$, $d^2T_1/dt^2 = 0$, $d^3T_1/dt^3 > 0$). The curve $d(t)$ shows an inflection at the point Ex, which characterizes the transition to low-rate reactions (Fig. 1a, b, c, d). Thus, according to the nonstationary model spontaneous extinction is determined by fulfilment of two conditions: $dT_1/dt = 0$ (steadiness) and $d^2T_1/dt^2 = 0$ (loss of the steadiness stability). The combustion time of a particle is determined by the lifetime of the high-temperature stage $t_{com} = t_{Ex} - t_{ind}$. Allowance for Stefan flow leads to a decrease in the combustion temperature and to an increase in the induction period, the combustion time t_{com}, and the critical particle diameter at which its spontaneous extinction occurs (Table 1). A comparison with experiment [5] points to the need to allow for Stefan flow when considering the heterogeneous particle combustion (Fig. 1).

To determine characteristics of the high- and low-temperature stationary stable states, the critical parameters of heterogeneous ignition and extinction of a carbon particle, we analyze the dependence of the diameter and heat and mass transfer coefficients of the particle on its temperature. Using the steady-state condition $dT_1/dt = 0$, from (1) we find a relationship between the diameter d and heat and mass transfer coefficients α and β and the stationary particle temperature in explicit form

$$\beta = \frac{2D}{d} = \frac{\alpha}{c_2\rho_2} = \frac{-B \pm \sqrt{B^2 - 4C}}{2}, \tag{3}$$

where

$$B = \sum_{i=1}^{2} k_i + P_{sf}\left[1 + \frac{T_1 + T_2}{2(T_1 - T_2)}\right] + \frac{\varepsilon\sigma(T_1^4 - T_w^4)}{c_2\rho_2(T_1 - T_2)} - \frac{\left(\sum_{i=1}^{2} k_i q_i\right)\rho_2 C_{1\infty}}{c_2\rho_2(T_1 - T_2)};$$

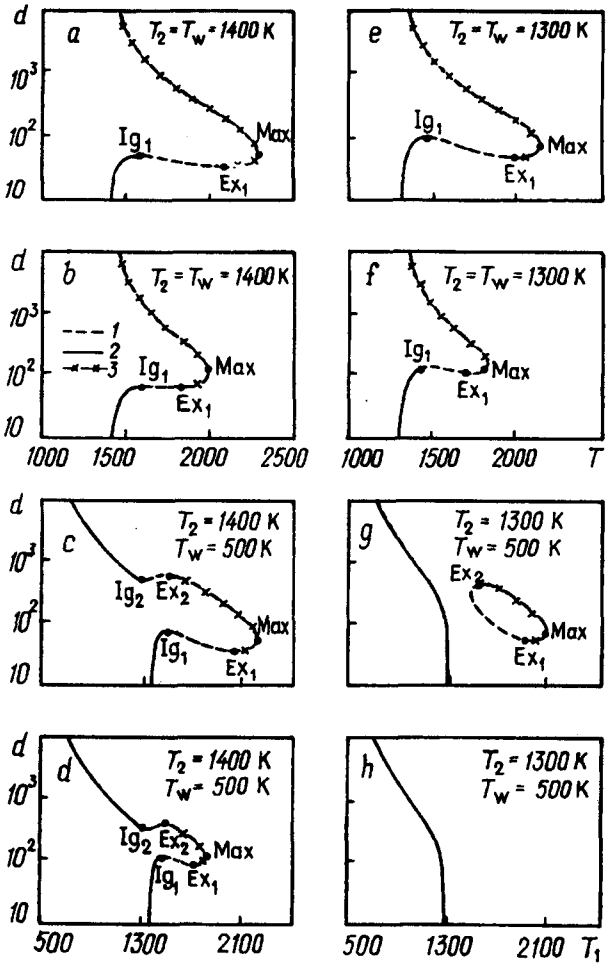

Fig. 2. Particle diameter versus stationary temperature at $C_{1\infty} = 0.23$ (a, c, e, g without allowance for Stefan flow; b, d, f, h, with allowance for it): 1) $d^*_{Ig}(T_{in})$ for ignition; 2) $d(T_1)$ for oxidation; 3) $d(T_{com})$ for particle combustion.

$$C = \frac{\varepsilon\sigma\,(T_1^4 - T_w^4)}{c_2\rho_2\,(T_1 - T_2)}\left(\sum_{i=1}^{2} k_i + P_{sf}\right).$$

Figure 2 shows the dependences $d(T_1)$ at gas temperatures $T_2 = 1300$ K and 1400 K and wall temperatures $T_w = T_2$ and $T_w = 500$ K to determine the contributions of radiation heat losses and Stefan flow. Extrema on the curves $d(T_1)$ determine unstable stationary regimes: 1) points Ig_1 and Ig_2 correspond to ignition; 2) points Ex_1 and Ex_2 indicate extinction of a particle. The extremum condition $\partial d/\partial T_1 = 0$ or $\partial\beta/\partial T_1 = 0$, $\partial\alpha/\partial T_1 = 0$ is equivalent to contact of the curves $Q_{ch}(T_1)$ and $Q_{h.r}(T_1)$:

$$\partial Q_{ch}/\partial T_1 = \partial Q_{h.r}/\partial T_1\,,\quad Q_{h.r} = Q_{\lambda,sf} + Q_r\,. \tag{4}$$

The branches connecting points Ig_1 and Ex_1 and Ig_2 and Ex_2 (the dashed curves) show the influence of the initial temperature of the particle on its critical diameter $d^*_{Ig}(T_{in})$ and is determined by the condition $\partial Q_{ch}/\partial T_1 > \partial Q_{h.r}/\partial T_1$, which becomes (4) at $T_{in} = T_{1Ig}$ and $T_{in} = T_{1Ex}$.

With an increase in the wall temperature T_w, the distance between points Ig_2 and Ex_2 decreases, and at some values of $T_{w\gamma}$ the critical conditions of ignition and extinction degenerate. At $T_w = T_2$, a transition to the high-temperature branch occurs smoothly for arbitrarily large particle diameters.

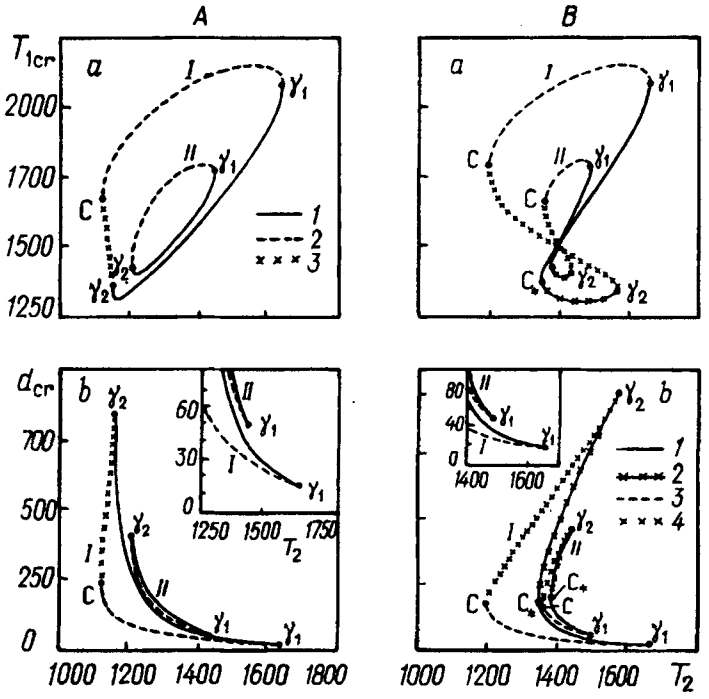

Fig. 3. Dependences of the critical particle temperatures (a) and diameters (b) on the gas temperature at $T_w = T_2$ (A) and $T_w = 500$ K (B) (I) without allowance for Stefan flow, II) with allowance for it): A: 1) T_{1Ig_1}, d_{Ig_1}; 2) T_{1Ex_1}, d_{Ex_1}; 3)T_{1Ex_2}, d_{Ex_2}; B: 1) T_{1Ig_1}, d_{Ig_1}; 2)T_{1Ig_2}, d_{Ig_2}; 3) T_{1Ex_1}, d_{Ex_1}; 4) T_{1Ex_2}, d_{Ex_2}

The solid curves $d(T_1)$ in Fig. 2 pertain to low-temperature stationary states. A transition to the high-temperature quasistationary states (the lines with crosses) at a wall temperature lower than the gas temperature $T_w < T_2$ (Fig. 2c, d) occurs if the initial particle diameter is in the interval $d_{Ig_1} < d_{in} < d_{Ex_2}$. For particles with a diameter larger than d_{Ig_2}, at first a transition to the low-temperature regime occurs. Then, as a result of decreasing particle diameter – this is a slow process – the particle enters the interval (d_{Ig_2}, d_{Ex_1}) and ignites. The combustion time of a particle with initial diameter $d_{in} > d_{Ig_2}$ is independent of its diameter.

The critical diameter of a particle (ignition) in the range of large diameters $(d_{Ig_2} < d^*_{Ig} < d_{Ex_2})$ increases with its initial temperature. This is explained by two reasons: an increase in the particle diameter causes a decrease in the heat flux, heating it at the expense of q_λ at $T_1 < T_2$, and leads to a decrease in the mass transfer coefficient and, consequently, Q_{ch} at $T_1 > T_2$.

A decrease in the gas temperature from $T_2 = 1400$ K by 100 K results in the fact that a transition to the high-temperatyure regime, ignoring Stefan flow, can occur only when the initial particle temperatures are higher than their critical values. The removal of heat and oxidant from a particle by the Stefan flow leads to only a low-temperature regime at $T_2 = 1300$ K and $T_w = 500$ K (Figs. 2 and 3).

The dependence of the stationary temperature of a particle on its initial diameter is hysteretic. Radiation heat losses are responsible for the presence of a second hysteresis loop in the region $d_{Ig_2} < d_{in} < d_{Ex_2}$. The presence of Stefan flow can make high-temperature stable states disappear under these conditions.

Figure 3 shows the critical temperatures and diameters of a particle versus the gas temperature determined by condition (4) with allowance for radiation heat losses ($T_w = T_2$, $T_w = 500$ K) with and without allowance for Stefan flow.

The behavior of the curves $d_{Ig_1}(T_2)$ and $d_{Ex_1}(T_2)$, $T_{1Ig_1}(T_2)$ and $T_{1Ex_1}(T_2)$ is similar to the case of $\varepsilon = 0$. Without allowance for radiation heat losses ($\varepsilon = 0$), the critical diameters d_{Ig} and d_{Ex} monotonically decrease and the difference between them decreases. At $T_2 = T_{2\gamma_1}$, the critical conditions of ignition and extinction $d_{Ig_1} = d_{Ex_1} = d_{\gamma_1}$, $T_{1Ig_1} = T_{1Ex_1} = T_{1\gamma_1}$ degenerate. Such behavior of the curves $d_{Ig_1}(T_2)$ and $d_{Ex_1}(T_2)$ is attributable to the

fact that a decrease in particle diameter entails an increase in heat losses due to heat conduction, and in order to restore the stationary state, it is necessary to increase the gas temperature.

The trend of the curves $d_{Ig_2}(T_2)$ and $d_{Ex_2}(T_2)$, $T_{1Ig_2}(T_2)$ and $T_{1Ex_2}(T_2)$ is determined by the radiation-induced heat losses from the particle to the walls of the reaction chamber whose temperature is $T_w < T_2$. In the range $d_C < d_{Ex_2} < d_{\gamma_2}$ and $d_{C_*} < d_{Ig_2} < d_{\gamma_2}$, with an increase in gas temperature, the critical particle diameters increase, while particle temperatures decrease (points C_* and C in Fig. 3 determine the critical gas temperatures, below which no particle ignition occurs due to a change in particle diameter and initial temperature). For the dependence $d_{Ig_2}(T_2)$ this is associated with two mechanisms: 1) in the region near the point C_*, $d_{Ig_2} > d_{C_*}$, an increase in d_{Ig_2} causes a decrease in the heat flux by conduction, heating of the particle, since $T_{1Ig_2} < T_2$; 2) in the region close to point γ_2, an increase in diameter leads to a decrease in the mass transfer coefficient and, consequently, in Q_{ch}.

The increase in d_{Ex_2} with T_2 is determined by the decrease in Q_{ch} due to a decrease in β. With an increase in the gas temperature, the critical values of d_{Ex_2} and d_{Ig_2}, T_{1Ex_2} and T_{1Ig_2} approach and the critical conditions of particle ignition and extinction, $d_{Ex_2} = d_{Ig_2} = d_{\gamma_2}$, $T_{1Ex_2} = T_{1Ig_2} = T_{1\gamma_2}$, degenerate.

The parameters of degeneracy of the critical conditions of ignition and extinction are determined by solution of a system of three equations [3]: $Q_{ch} = Q_{h.r}$, $\partial Q_{ch}/\partial T_1 = \partial Q_{h.r}/\partial T_1$, $\partial^2 Q_{ch}/\partial T_1^2 = \partial^2 Q_{h.r}/\partial T_1^2$. The last relation is equivalent to the condition that determines the critical transition of extrema on the curves of the regime parameters (particle diameter, gas temperature, oxidant concentration) versus the stationary particle temperature to the inflection point. This means that the area of the hysteresis loop is equal to zero, i.e., at $T_2 > T_{2\gamma_1}$ the transitions from the high-temperature to low-temperature stationary stable states and vice versa proceed without a jump. Stefan flow leads to a decrease in $T_{2\gamma_2}$ and $T_{2\gamma_1}$, d_{γ_2} and an increase in d_{γ_1}.

Radiation heat losses are responsible for the presence of limiting critical gas temperatures (points C and C_* in Fig. 3), at which $d_{Ig_1} = d_{Ig_2}$ and $d_{Ex_1} = d_{Ex_2}$. In the curves of $T_{2cr}(d)$, those are minimum points. At $T_2 < T_{2C}$, a transition to the high-temperature regime is impossible. In the gas temperature range $T_{2C} < T_2 < dT_{2C_*}$, particle ignites due to an increase in its initial temperature to a value higher than the critical one. The limiting critical gas temperatures and the corresponding particle diameters and temperatures are determied from the condition $\partial T_{2cr}/\partial(d) = 0$ or $\partial T_{2cr}/\partial\beta = 0$, which is equivalent to the equality

$$\frac{\partial Q_{ch}}{\partial\beta} = \frac{\partial Q_{h.r}}{\partial\beta}, \tag{5}$$

since $Q_{ch} = Q_{h.r}$ and $\partial Q_{ch}/\partial T_1 = \partial Q_{h.r}/\partial T_1$.

Using (5), we can represent the criterion determining points C and C_* as follows

$$\frac{2\lambda_2 (T_{1cr} - T_2)}{d\varepsilon\sigma (T_{1cr}^4 - T_w^4)} = \frac{\sum_{i=1}^{2} k_i + P_{sf}}{\beta} \tag{6}$$

or

$$\frac{\rho_2 C_{1\infty} \sum_{i=1}^{2} q_i k_i - \frac{1}{2} P_{sf} c_2 \rho_2 (T_{1cr} + T_2)}{\varepsilon\sigma (T_{1cr}^4 - T_w^4)} = \left[1 + \frac{\sum_{i=1}^{2} k_i + P_{sf}}{\beta}\right]^2. \tag{7}$$

At point C, $(\sum_{i=1}^{2} k_i + P_{sf})/\beta = 2$, i.e., upon extinction the radiation heat losses are comparable to the heat losses by conduction. For point C_*, $(\sum_{i=1}^{2} k_i + P_{sf})/\beta \simeq 1/8$. Then from (6) it follows that $T_{1cr} \simeq T_2$, $T_2 = T_{1C_*}$. The value of T_{2C_*} is determined from an approximate formula derived from (6) and (7):

$$\frac{\rho_2 C_{1\infty} \sum_{i=1}^{2} q_i k_i - P_{sf} c_2 T_{2C_*} \rho_2}{\varepsilon\sigma (T_{2C_*}^4 - T_w^4)} = 1 , \tag{8}$$

where $k_i = k_{0i} \exp(-E_i/RT_{2C_*})$, i.e., the heat losses are fully caused by radiation and Stefan flow. As is seen from (8), at a given oxidant concentration, Stefan flow leads to an increase in the limiting gas temperature T_{2C_*} below which particle self-ignition is impossible.

Thus, it has been established that allowance for radiation and Stefan flow reveals new qualitative and quantitative regularities in the heterogeneous combustion of a carbon particle with concurrent chemical reactions proceeding on its surface.

NOTATION

T, temperature, K; t, time, sec; ρ, density, kg/m^3; c, specific heat, J/kg·K; d, particle diameter, m; λ, thermal conductivity, W/m·K; ε, particle emissivity; v, Stefan flow velocity, m/sec; $C_{1\infty}$, relative mass concentration of oxygen; μ_i, molar mass, kg/mole; k_1, k_2, rate constants of the first and the second reactions, m/sec; k, total constant of chemical reaction rates, m/sec; k_{01}, k_{02}, preexponential of the first and the second chemical reactions, respectively, m/sec; E_1, E_2, activation energy of reactions (I) and (II), respectively, J/mole; D, diffusion coefficient, m^2/sec; Q_{ch}, surface power of heat release, W/m^2; $Q_{\lambda,sf}$, specific heat flux due to heat conduction and Stefan flow, W/m^2; Q_r, mass transfer coefficient, m/sec; α, heat transfer coefficient, W/m^2·K; Ω_1, Ω_2, relative mass stoichiometric coefficients for the first and second reactions. Indices: 1, particle; 2, gas; w, wall; sf, Stefan; ∞, at infinite removal; in, initial; λ, thermal conductivity, r, radiation; ch, chemical; h.r., heat removal; j = 1, O_2; 2, CO_2; 3, CO; 4, N_2; 5, C; cr, critical; Ig, ignition; Ex, extinction; com, combustion; ind, induction; γ, degeneracy; max, maximum; eff, effective.

REFERENCES

1. S. G. Orlovskaya and V. V. Kalinchak, Fiz. Goren. Vzryva, 26, No. 1, 115-118 (1990).
2. V. V. Kalinchak, S. G. Orlovskaya, and A. I. Kalinchak, in: Proc. of the Second Minsk Int. Forum, Vol. 3 (1992), pp. 11-15.
3. V. V. Kalinchak, S. G. Orlovskaya, and A. I. Kalinchak, Inzh.-Fiz. Zh., 62, No. 3, 436-442 (1992).
4. V. V. Kalinchak and A. V. Dubinskii, Inzh.-Fiz. Zh., 68, No. 4, 576-582 (1994).
5. V. I. Babii and Yu. F. Kuvaev, Coal Dust Combustion and Calculation of a Dust-Laden Coal Flare [in Russian], Moscow (1986).
6. V. V. Pomerantsev (ed.), Fundamentals of the Practical Theory of Combustion [in Russian], Leningrad (1986).